

Supporting Information

Reductive Formation of a Vanadium(IV/V) Oxide Cluster Complex $[V_8O_{19}(4,4'\text{-}^t\text{Bubpy})_3]$ Having a C_3 -Symmetric Propeller-Shaped Nonionic V_8O_{19} Core

Yuta Inoue,[†] Shintaro Kodama,^{*,†,‡} Nobuto Taya,[†] Hirohiko Sato,[§] Katsuyoshi Oh-ishi,[†] and Youichi Ishii^{*,†}

[†]Department of Applied Chemistry, Faculty of Science and Engineering, Chuo University, 1-13-27 Kasuga, Bunkyo-ku, Tokyo 112-8551, Japan

[§]Department of Physics, Faculty of Science and Engineering, Chuo University, 1-13-27 Kasuga, Bunkyo-ku, Tokyo 112-8551, Japan

[‡]Present address: Department of Applied Chemistry, Graduate School of Engineering, Osaka Prefecture University, 1-1 Gakuen-cho, Nakaku, Sakai, Osaka 599-8531, Japan

Contents

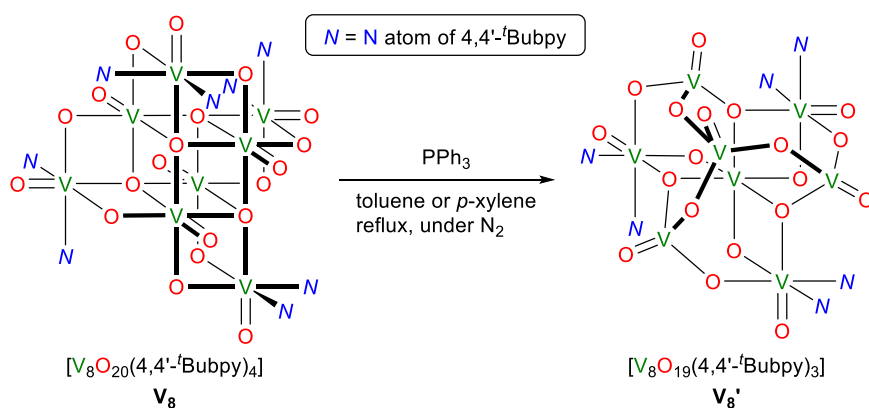
General Considerations	S2
Experimental Procedures	S2—S6
X-ray Diffraction Studies	S7—S14
Results of SQUID Measurements	S15
Results of TG-DTA analysis	S16
References	S17

General Considerations

Experimental manipulations for the reductive conversion of vanadium(V) oxide cluster complexes were carried out in a dried glass vessel under a nitrogen atmosphere by standard Schlenk techniques. ^1H (500 MHz) and $^{31}\text{P}\{^1\text{H}\}$ (202 MHz) NMR spectra were recorded on a JEOL ECA-500 spectrometer. Chemical shifts are reported in δ , referenced to the residual ^1H signal of a deuterated solvent as an internal standard, to the ^{31}P signal of PPh_3 ($\delta -5.65$) as an external standard. IR spectra were recorded on a JASCO FT/IR-410 spectrometer using KBr pellets. Elemental analyses were conducted on a Perkin Elmer 2400 series II CHN analyzer. Magnetic susceptibility measurements were performed using a Quantum Design MPMS-XL superconducting quantum interference device (SQUID) magnetometer. Diamagnetic corrections were evaluated using Pascal's constants.^{S1} Vanadium(V) oxide cluster complexes, $[\text{V}_8\text{O}_{20}(4,4'\text{-}^t\text{Bubpy})_4]$ (V_8), $[\text{V}_4\text{O}_8(\text{OMe})_4(4,4'\text{-}^t\text{Bubpy})_2]$ (V_4), and $[\text{V}_7\text{O}_{17}(\text{OEt})(4,4'\text{-}^t\text{Bubpy})_3]$ ($\text{V}_7\text{-Et}$), were synthesized according to the previously reported procedures.^{S2} Unless otherwise noted, reagents were purchased from commercial source and used without further purification.

Experimental Procedures

Reductive Formation of Octanuclear Vanadium(IV/V) Oxide Cluster Complex V_8' from V_8

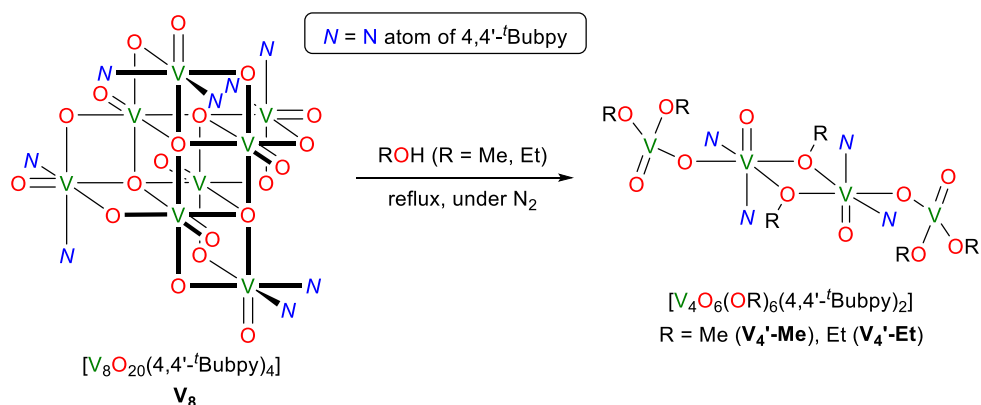


$[\text{V}_8\text{O}_{19}(4,4'\text{-}^t\text{Bubpy})_3] \cdot 0.42\text{C}_7\text{H}_8$ ($\text{V}_8' \cdot 0.42\text{C}_7\text{H}_8$): Complex $\text{V}_8 \cdot \text{CH}_2\text{Cl}_2$ (568.9 mg, 0.30 mmol) and PPh_3 (632.1 mg, 2.41 mmol) in toluene (30.0 mL) were heated at reflux for 5 min under N_2 to form a dark green suspension. This suspension was filtered and allowed to stand overnight at room temperature to deposit dark blue crystals suitable for X-ray analysis. The crystals were collected by filtration, washed with toluene, and dried under vacuum to give $\text{V}_8' \cdot 0.42\text{C}_7\text{H}_8$ (an empirical formula)

(85.2 mg, 18% yield based on vanadium). Comparison of this empirical formula with the structure obtained by the X-ray analysis ($V_8 \cdot 3C_7H_8$) indicates that most parts of solvent molecules (toluene) in the crystals were lost during the drying process. IR (KBr, cm^{-1}) 2964 (ν_{CH}), 1619 ($\nu_{C=C, C=N}$), 1413 ($\nu_{C=C, C=N}$), 979 ($\nu_{V=O}$), 849 (ν_{CH}), 812 (ν_{CH}), 770 (ν_{CH}); Anal. Calcd for $C_{54}H_{72}N_6O_{19}V_8 \cdot 0.42C_7H_8$: C, 43.97; H, 4.88; N, 5.40. Found: C, 43.96; H, 4.80; N, 5.20%.

$[V_8O_{19}(4,4'\text{-}^t\text{Bubpy})_3] \cdot 1.28C_8H_{10}$ ($V_8' \cdot 1.28C_8H_{10}$): This complex was obtained by a procedure similar to that for the synthesis of $V_8' \cdot 0.42C_8H_{10}$ using $V_8 \cdot CH_2Cl_2$ (565.5 mg, 0.30 mmol), PPh_3 (636.7 mg, 2.43 mmol), and *p*-xylene (30.0 mL). Dark blue crystals (33.8 mg, 7% yield based on vanadium) deposited from the filtered reaction mixture were collected by filtration, washed with *p*-xylene, and dried in vacuo to give $V_8' \cdot 1.28C_8H_{10}$ (an empirical formula). Comparison of this formula with the structure obtained by the X-ray analysis ($V_8' \cdot 3C_8H_{10}$) indicates that most parts of solvent molecules (*p*-xylene) in the crystals were lost during the drying process. IR (KBr, cm^{-1}) 2966 (ν_{CH}), 1619 ($\nu_{C=C, C=N}$), 1413 ($\nu_{C=C, C=N}$), 980 ($\nu_{V=O}$), 848 (ν_{CH}), 811 (ν_{CH}), 767 (ν_{CH}); Anal. Calcd for $C_{54}H_{72}N_6O_{19}V_8 \cdot 1.28C_8H_{10}$: C, 46.69; H, 5.17; N, 5.09. Found: C, 46.67; H, 5.25; N, 4.75%.

Reductive Formation of Tetranuclear Vanadium(IV/V) Oxide Cluster Complex V_4' from V_8



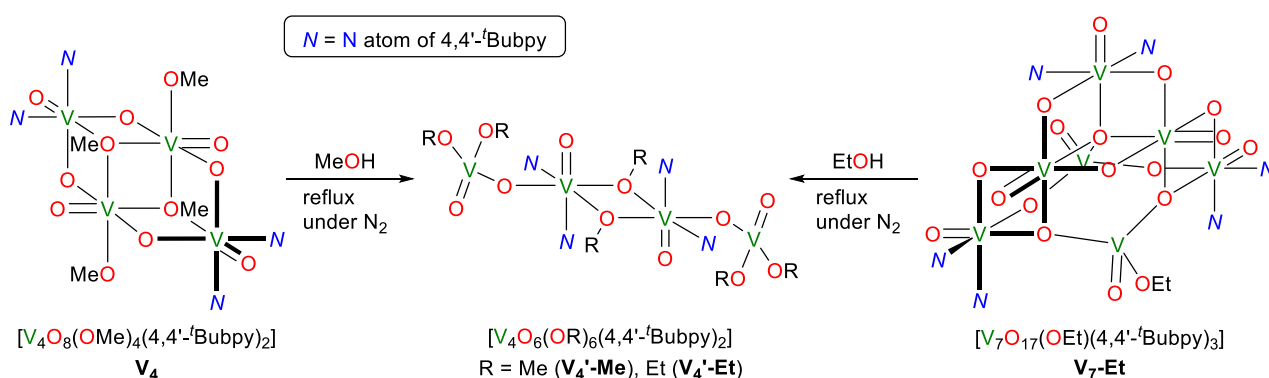
$[V_4O_6(OMe)_6(4,4'\text{-}^t\text{Bubpy})_2]$ ($V_4'\text{-}Me$): Complex $V_8 \cdot CH_2Cl_2$ (541.8 mg, 0.29 mmol) in MeOH (30.0 mL) was heated at reflux for 24 h under nitrogen to generate a green suspension. The green powder deposited was collected by filtration and washed with MeOH to afford $V_4'\text{-}Me$ (329.5 mg, 56% yield based on vanadium). IR (KBr, cm^{-1}) 2963 (ν_{CH}), 1617 ($\nu_{C=C, C=N}$), 1410 ($\nu_{C=C, C=N}$), 962

($\nu_{V=O}$), 956 ($\nu_{V=O}$), 886 (ν_{CH}), 848 (ν_{CH}), 800 (ν_{CH}); Anal. Calcd for $C_{42}H_{66}N_4O_{12}V_4$: C, 49.32; H, 6.50; N, 5.48. Found: C, 49.07; H, 6.70; N, 5.47%.

Crystals of V_4' -Me suitable for X-ray analysis were obtained as follows: complex $V_8 \cdot CH_2Cl_2$ (44.6 mg, 0.024 mmol) in MeOH (5.0 mL) were heated at reflux for 19 h under nitrogen, and the resulting dark green suspension was filtered. The dark green filtrate was allowed to stand overnight at room temperature to deposit dark green crystals, which were suitable for X-ray analysis. The crystals were collected by filtration and washed with MeOH to afford V_4' -Me (4.9 mg, 10% yield based on vanadium).

$[V_4O_6(OEt)_6(4,4'\text{-}^t\text{Bubpy})_2]$ (V_4' -Et): Complex $V_8 \cdot CH_2Cl_2$ (542.0 mg, 0.29 mmol) in EtOH (30.0 mL) was heated at reflux for 24 h under nitrogen, and the resulting dark orange solution was filtered through a celite pad and allowed to stand for 4 days at room temperature to deposit dark orange crystals which were suitable for X-ray analysis. The crystals were collected by filtration and washed with EtOH to afford V_4' -Et (336.8 mg, 53% yield based on vanadium). IR (KBr, cm^{-1}) 2965 (ν_{CH}), 1616 ($\nu_{C=C, C=N}$), 1410 ($\nu_{C=C, C=N}$), 968 ($\nu_{V=O}$), 956 ($\nu_{V=O}$), 888 (ν_{CH}), 850 (ν_{CH}), 799 (ν_{CH}); Anal. Calcd for $C_{48}H_{78}N_4O_{12}V_4$: C, 52.08; H, 7.10; N, 5.06. Found: C, 51.97; H, 7.29; N, 5.01%.

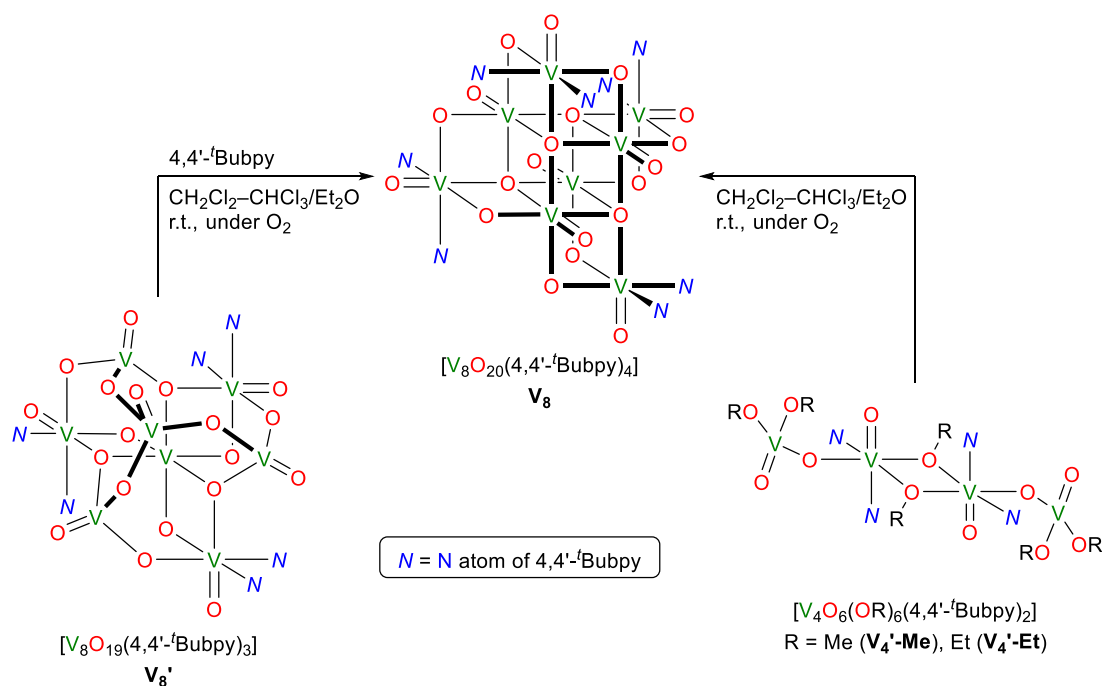
Reductive Formation of V_4' from V_4 or V_7 -Et



Conversion of V_4 to V_4' -Me: Complex $V_4 \cdot 2H_2O$ (31.6 mg, 0.031 mmol) in MeOH (3.0 mL) was heated at reflux for 19 h under N_2 . The resulting dark green solution was allowed to stand for 4 days at room temperature to deposit dark green crystals. The crystals were collected by filtration and washed with MeOH to afford V_4' -Me (13.6 mg, 43% yield based on vanadium).

Conversion of V₇-Et to V₄'-Et: Complex V₇-Et (149.9 mg, 0.10 mmol) in EtOH (5.0 mL) was heated at reflux for 21 h under N₂. The resulting dark orange solution was allowed to stand for 4 days at room temperature to deposit dark orange crystals. The crystals were collected by filtration and washed with EtOH to afford V₄'-Et (72.3 mg, 37% yield based on vanadium).

Oxidative Formation of V₈ from V₈' or V₄'

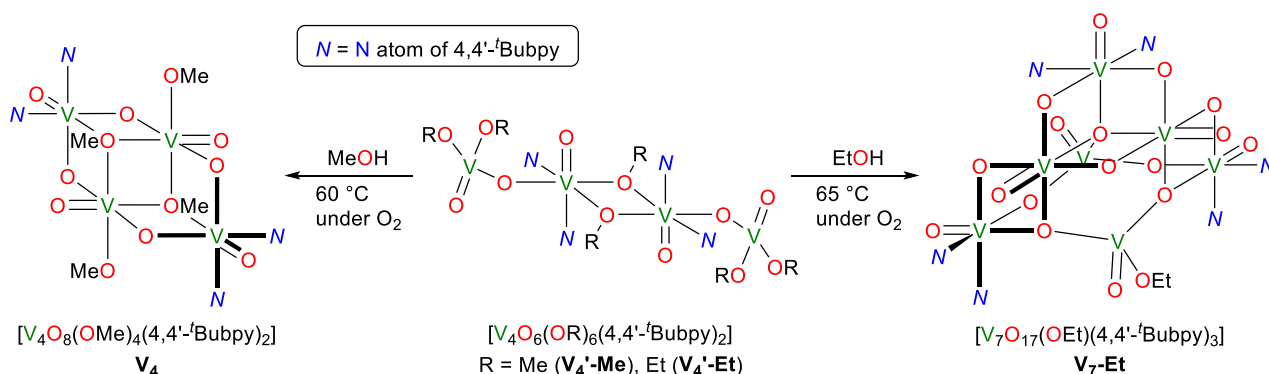


Conversion of V₈' to V₈: To a CHCl₃–CH₂Cl₂ (7.0 mL) solution (v/v = 1:1) of V₈'·0.42toluene (75.2 mg, 0.048 mmol) and 4,4'-t-Bubpy (13.2 mg, 0.049 mmol) was added Et₂O (14.0 mL), and the resulting brown suspension was stirred at room temperature for 2 days under O₂. The resulting yellow suspension was evaporated and dissolved in CH₂Cl₂–Et₂O mixture (v/v = 1:1). The yellow powder thus obtained was collected and washed with CH₂Cl₂ to afford V₈·CH₂Cl₂ (70.0 mg, 77% yield based on vanadium).

Conversion of V₄'-Me to V₈: To a CHCl₃–CH₂Cl₂ (7.3 mL) solution (v/v = 1:1) of V₄'-Me (51.2 mg, 0.050 mmol) was added Et₂O (14.6 mL), and the resulting brown solution was stirred at room temperature for 2 days under O₂. The yellow suspension was evaporated and dissolved in CH₂Cl₂–Et₂O mixture (v/v = 1:1). The resulting yellow powder thus obtained was collected and washed with CH₂Cl₂ to afford V₈·CH₂Cl₂ (36.5 mg, 77% yield based on vanadium).

Conversion of V₄'-Et to V₈: To a CHCl₃–CH₂Cl₂ (7.3 mL) solution (v/v = 1:1) of V₄'-Et (55.3 mg, 0.050 mmol) was added Et₂O (14.6 mL), and the resulting brown solution was stirred at room temperature for 2 days under O₂. The resulting yellow suspension was evaporated and dissolved in CH₂Cl₂–Et₂O mixture (v/v = 1:1). The yellow powder thus obtained was collected and washed with CH₂Cl₂ to afford V₈·CH₂Cl₂ (30.5 mg, 65% yield based on vanadium).

Oxidative Formation of V₄ or V₇-Et from V₄'



Conversion of V₄'-Me to V₄: V₄'-Me (51.0 mg, 0.050 mmol) in MeOH (2.5 mL) was heated at 60 °C for 2 days under O₂. The resulting brown solution was allowed to stand overnight at room temperature to deposit yellow crystals. The crystals were collected by filtration and washed with MeOH to afford V₄ (13.0 mg, 26% yield based on vanadium).

Conversion of V₄'-Et to V₇-Et: V₄'-Et (110.4 mg, 0.10 mmol) in EtOH (2.5 mL) was heated at 65 °C for 2 days under O₂ to form a yellow-green suspension. The yellow-green crystalline precipitates were collected, washed with EtOH, and dried in vacuo to afford V₇-Et as a yellow-green powder (64.4 mg, 76% yield based on vanadium).

X-ray Diffraction Studies

Diffraction data for $\text{V}_8' \cdot 3\text{C}_7\text{H}_8$, $\text{V}_8' \cdot 3\text{C}_8\text{H}_{10}$, $\text{V}_4' \cdot \text{Me}$, and $\text{V}_4' \cdot \text{Et}$ were collected on a Rigaku VariMax with a Saturn CCD diffractometer using multilayer mirror monochromated Mo-K α radiation ($\lambda = 0.71075 \text{ \AA}$) at $-180 \text{ }^\circ\text{C}$. Intensity data were corrected for Lorentz and polarization effects and for an empirical absorption.^{S3} All calculations were performed using the *CrystalStructure*^{S4} crystallographic software package except for refinements, which was performed using SHELXL Version 2016/6.^{S5} The structures were solved by direct methods (SHELXS Version 2013/1)^{S6} and expanded using Fourier techniques. Non-hydrogen atoms were refined on F^2 anisotropically by full-matrix least-squares techniques. Hydrogen atoms were placed at the calculated positions with fixed isotropic parameters. For $\text{V}_8' \cdot 3\text{C}_7\text{H}_8$, solvent molecules (toluene) were badly disordered, and the structure of $\text{V}_8' \cdot 3\text{C}_7\text{H}_8$ was refined without these solvents using PLATON Squeeze technique,^{S6} which reported that the volume of total potential solvent accessible void is 574 \AA^3 per unit cell, and estimated number of electrons within the void is 109 electrons/cell. Expected volumes for small molecules (e.g. toluene) are $100\text{--}300 \text{ \AA}^3$, and toluene has 50 electrons per molecule. From these results, we assumed that the unit cell contains 2 molecules of toluene (100 electrons). There is a level B alert due to the disorder of a solvent molecule (toluene), but it does not affect the final structure determination. For $\text{V}_8' \cdot 3\text{C}_8\text{H}_{10}$, there is a level B alert: Missing # of FCF reflections below Theta(Min). However, data completeness of 96.3% is enough for structure determination. For $\text{V}_4' \cdot \text{Et}$, hydrogen atoms of bridged ethoxide groups were not included in the refinements. Details of the X-ray diffraction study are summarized in Table S1. ORTEP drawings of $\text{V}_8' \cdot 3\text{C}_8\text{H}_{10}$, $\text{V}_4' \cdot \text{Me}$, and $\text{V}_4' \cdot \text{Et}$ are shown in Figures S1–3 and selected interatomic distances and angles are listed in Tables S2–4. Results of bond valence sum (BVS) calculations for vanadium atoms of $\text{V}_8' \cdot 3\text{C}_7\text{H}_8$, $\text{V}_8' \cdot 3\text{C}_8\text{H}_{10}$, $\text{V}_4' \cdot \text{Me}$, and $\text{V}_4' \cdot \text{Et}$ are shown in Table S5.

Table S1. X-ray crystallographic data for $V_8' \cdot 3C_7H_8$, $V_8' \cdot 3C_8H_{10}$, $V_4' \cdot Me$, and $V_4' \cdot Et$

	$V_8' \cdot 3C_7H_8$	$V_8' \cdot 3C_8H_{10}$	$V_4' \cdot Me$	$V_4' \cdot Et$
CCDC	1828015	1828016	1828017	1828019
chemical formula	$C_{75}H_{96}N_6O_{19}V_8$	$C_{78}H_{102}N_6O_{19}V_8$	$C_{42}H_{66}N_4O_{12}V_4$	$C_{48}H_{78}N_4O_{12}V_4$
formula weight	1793.14	1835.22	1022.77	1106.93
dimension of crystals	0.230×0.090×0.085	0.234×0.113×0.040	0.213×0.137×0.106	0.280×0.231×0.124
crystal system	trigonal	triclinic	monoclinic	monoclinic
space group	P-3 (#147)	P-1 (#2)	P2 ₁ /c (#14)	P2 ₁ /c (#14)
<i>a</i> , Å	20.323(3)	11.6193(17)	10.739(7)	10.609(4)
<i>b</i> , Å	20.323(3)	15.836(3)	21.314(12)	22.256(7)
<i>c</i> , Å	12.3450(18)	23.758(3)	10.433(7)	11.793(4)
α , deg	90.0000	85.348(5)	90.0000	90.0000
β , deg	90.0000	77.919(4)	98.259(10)	102.777(5)
γ , deg	120.0000	87.030(5)	90.0000	90.0000
<i>V</i> , Å ³	4415.5(11)	4257.8(11)	2363(2)	2715.5(16)
<i>Z</i>	2	2	2	2
ρ_{calcd} , g cm ⁻³	1.349	1.431	1.437	1.354
<i>F</i> (000)	1848.00	1896.00	1068.00	1164.00
μ , cm ⁻¹	8.719	9.059	8.283	7.265
trans. factors range	0.911–0.929	0.783–0.964	0.836–0.916	0.606–0.914
index ranges	$-26 \leq h \leq 26$	$-14 \leq h \leq 15$	$-13 \leq h \leq 13$	$-13 \leq h \leq 13$
	$-26 \leq k \leq 26$	$-20 \leq k \leq 20$	$-24 \leq k \leq 27$	$-27 \leq k \leq 27$
	$-16 \leq l \leq 15$	$-30 \leq l \leq 30$	$-13 \leq l \leq 13$	$-15 \leq l \leq 15$
no. rflns measured	36793	35310	18716	21853
no. unique rflns	6749	18777	5397	6117
R_{int}	0.0875	0.0555	0.0868	0.0643
no. rflns ($I > 2\sigma(I)$)	5546	13300	4063	4576
no. params refined	325	1000	280	313
$R1$ ($I > 2\sigma(I)$) ^a	0.0793	0.0703	0.0916	0.0807
R (All cata)	0.0965	0.1014	0.1199	0.1012
$wR2$ (All cata) ^b	0.1839	0.1619	0.2126	0.2500
GOF ^c	1.133	1.086	1.120	1.069
max diff peak/hole, e Å ⁻³	0.60/−0.47	0.51/−0.68	0.73/−0.71	2.16/−1.37

^a $RI = \sum||F_o| - |F_c|| / \sum|F_o|$. ^b $wR2 = [\sum\{w(F_o^2 - F_c^2)^2\} / \sum w(F_o^2)^2]^{1/2}$, $w = 1 / [\sigma^2 F_o^2 + (aP)^2 + bP]$ (*a* and *b* are constants suggested by the refinement program; $P = [\max(F_o^2, 0) + 2F_c^2] / 3$). ^c $GOF = [\sum w(F_o^2 - F_c^2)^2 / (N_{\text{obs}} - N_{\text{params}})]^{1/2}$.

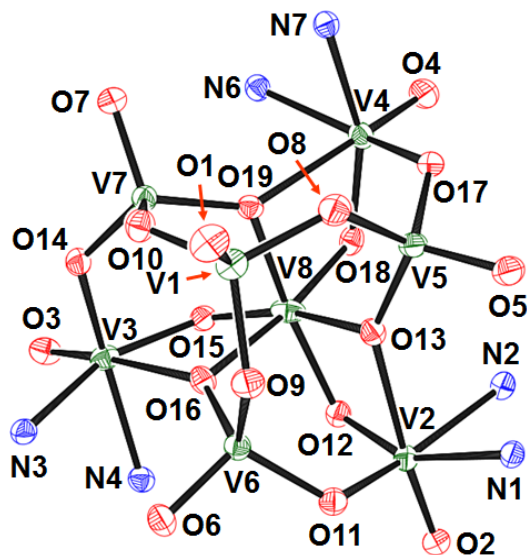


Figure S1. Crystal structure of $V_8' \cdot 3C_8H_{10}$ with numbered atoms. Ellipsoids are shown at the 50% probability level. H and C atoms are omitted for clarity.

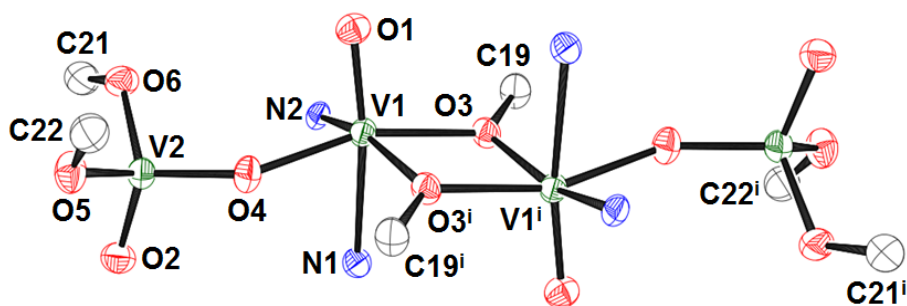


Figure S2. Crystal structure of V_4' -Me with numbered atoms. Ellipsoids are shown at the 50% probability level. H and C atoms except for C19, C21, C22, C19ⁱ, C21ⁱ, and C22ⁱ are omitted for clarity. Symmetry operators: (i) $-X + 1, -Y, -Z$.

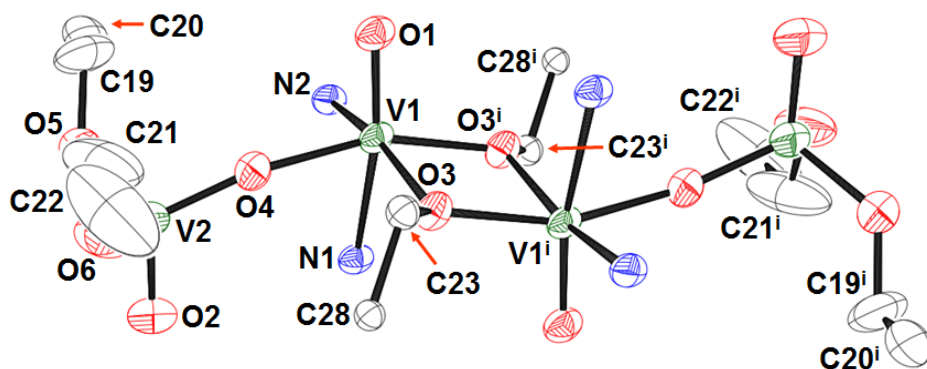


Figure S3. Crystal structure of V_4' -Et with numbered atoms. Ellipsoids are shown at the 50% probability level. H and C atoms except for C19, C20, C21, C22, C23, C28, C19ⁱ, C20ⁱ, C21ⁱ, C22ⁱ, C23ⁱ, and C28ⁱ are omitted for clarity. Symmetry operators: (i) $-X + 1, -Y, -Z + 1$.

Table S2. Selected interatomic distances (Å) and angles (deg) for $V_8' \cdot 3C_8H_{10}$

Interatomic distances (Å)			
V1–O1	1.598(3)	V1–O8	1.758(3)
V1–O9	1.770(3)	V1–O10	1.766(3)
V2–O2	1.607(3)	V2–O11	1.865(3)
V2–O12	1.734(3)	V2–O13	2.269(3)
V2–N1	2.169(4)	V2–N2	2.144(3)
V3–O3	1.602(3)	V3–O14	1.906(3)
V3–O15	1.860(3)	V3–O16	2.294(3)
V3–N3	2.143(4)	V3–N4	2.134(3)
V4–O4	1.592(3)	V4–O17	1.902(3)
V4–O18	1.879(3)	V4–O19	2.369(3)
V4–N5	2.139(3)	V4–N6	2.132(4)
V5–O5	1.601(3)	V5–O8	1.840(3)
V5–O13	1.746(3)	V5–O17	1.723(3)
V6–O6	1.602(3)	V6–O9	1.825(3)
V6–O11	1.766(2)	V6–O16	1.731(3)
V7–O7	1.615(3)	V7–O10	1.824(3)
V7–O14	1.729(3)	V7–O19	1.750(3)
V8–O12	1.951(2)	V8–O13	2.070(3)
V8–O15	1.805(3)	V8–O16	2.104(3)
V8–O18	1.794(3)	V8–O19	1.996(3)
V2···V8	3.0779(11)	V3···V8	3.0912(11)
V4···V8	3.0857(11)		
Angles (deg)			
V1–O8–V5	128.23(16)	V2–O11–V6	124.05(16)
V2–O12–V8	113.13(15)	V2–O13–V5	144.40(15)
V2–O13–V8	90.26(11)	V3–O15–V8	115.01(16)
V3–O16–V8	89.19(11)	V4–O18–V8	114.29(15)
V4–O19–V8	89.57(10)		

Table S3. Selected interatomic distances (Å) and angles (deg) for **V₄'-Me**

Interatomic distances (Å)			
V1–O1	1.609(4)	V1–O3	2.012(3)
V1–O3 ⁱ	1.968(4)	V1–O4	1.976(4)
V1–N1	2.309(4)	V1–N2	2.144(4)
V2–O2	1.617(4)	V2–O4	1.687(4)
V2–O5	1.792(4)	V2–O6	1.794(4)
V1⋯V1 ⁱ	3.140(2)		

Angles (deg)			
O3–V1–O3 ⁱ	75.83(15)	V1–O3–V1 ⁱ	104.17(17)
V1–O4–V2	144.4(2)		

Symmetry operators: (i) – X + 1, – Y, – Z.

Table S4. Selected interatomic distances (Å) and angles (deg) for **V₄'-Et**

Interatomic distances (Å)			
V1–O1	1.604(3)	V1–O3	1.970(3)
V1–O3 ⁱ	2.005(2)	V1–O4	1.973(3)
V1–N1	2.281(3)	V1–N2	2.164(3)
V2–O2	1.625(4)	V2–O4	1.688(3)
V2–O5	1.770(4)	V2–O6	1.792(4)
V1⋯V1 ⁱ	3.1411(13)		

Angles (deg)			
O3–V1–O3 ⁱ	75.57(11)	V1–O3–V1 ⁱ	104.43(13)
V1–O4–V2	161.51(18)		

Symmetry operators: (i) – X + 1, – Y, – Z + 1.

Table S5. BVS calculations for vanadium atoms of $\mathbf{V}_8' \cdot 3\text{C}_7\text{H}_8$, $\mathbf{V}_8' \cdot 3\text{C}_8\text{H}_{10}$, $\mathbf{V}_4' \text{-Me}$, and $\mathbf{V}_4' \text{-Et}$ ^a

V complex		V1	V2	V3	V4	V5	V6	V7	V8
$\mathbf{V}_8' \cdot 3\text{C}_7\text{H}_8$	V(IV)	4.82	4.54	4.72	4.01	–	–	–	–
	V(V)	5.08	4.74	4.97	4.22	–	–	–	–
$\mathbf{V}_8' \cdot 3\text{C}_8\text{H}_{10}$	V(IV)	4.81	4.73	4.36	4.34	4.79	4.73	4.73	4.00
	V(V)	5.07	4.93	4.54	4.51	5.04	4.98	4.98	4.21
$\mathbf{V}_4' \text{-Me}$	V(IV)	4.10	4.82	–	–	–	–	–	–
	V(V)	4.29	5.08	–	–	–	–	–	–
$\mathbf{V}_4' \text{-Et}$	V(IV)	4.14	4.85	–	–	–	–	–	–
	V(V)	4.32	5.11	–	–	–	–	–	–

^a BVS calculations were conducted using X-ray data of $\mathbf{V}_8' \cdot 3\text{C}_7\text{H}_8$ (Figure 2 in the manuscript), $\mathbf{V}_8' \cdot 3\text{C}_8\text{H}_{10}$ (Table S2), $\mathbf{V}_4' \text{-Me}$ (Table S3), and $\mathbf{V}_4' \text{-Et}$ (Table S4). Bond valence parameters: V(IV)–O (1.784 Å), V(V)–O (1.803 Å), and V–N (1.86 Å).^{S7}

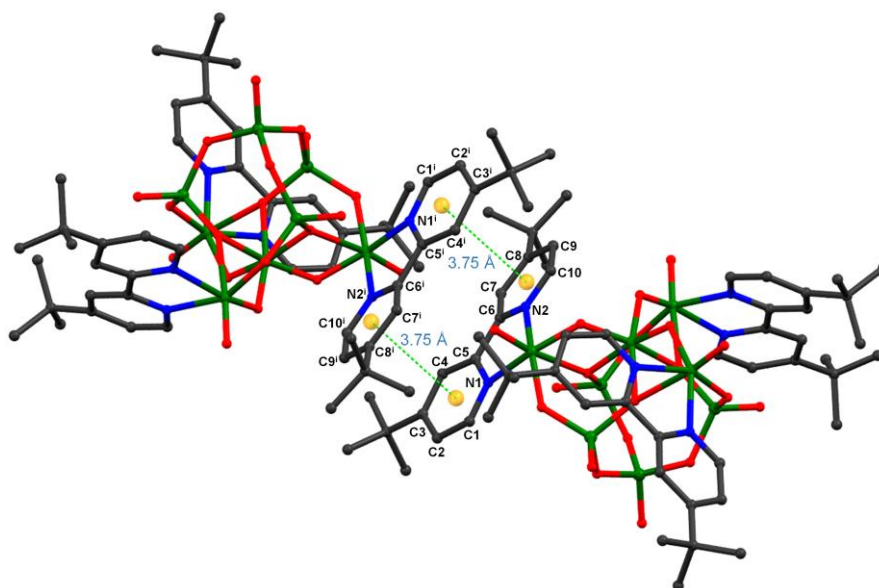


Figure S4. π - π interactions between pyridine rings of $V_8' \cdot 3C_7H_8$ with a centroid-centroid distance of 3.75 Å. Symmetry operators: (i) $1 - X, 1 - Y, -Z$.

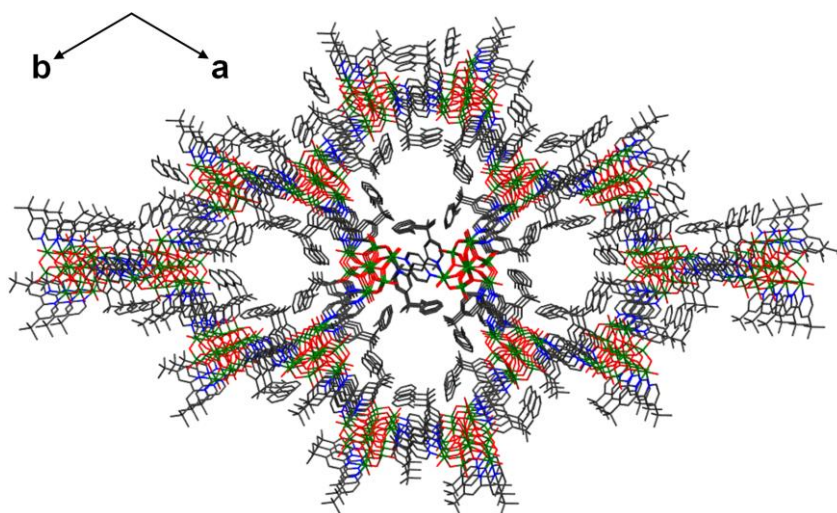


Figure S5. Crystal packing view of $V_8' \cdot 3C_7H_8$ along the c -axis.

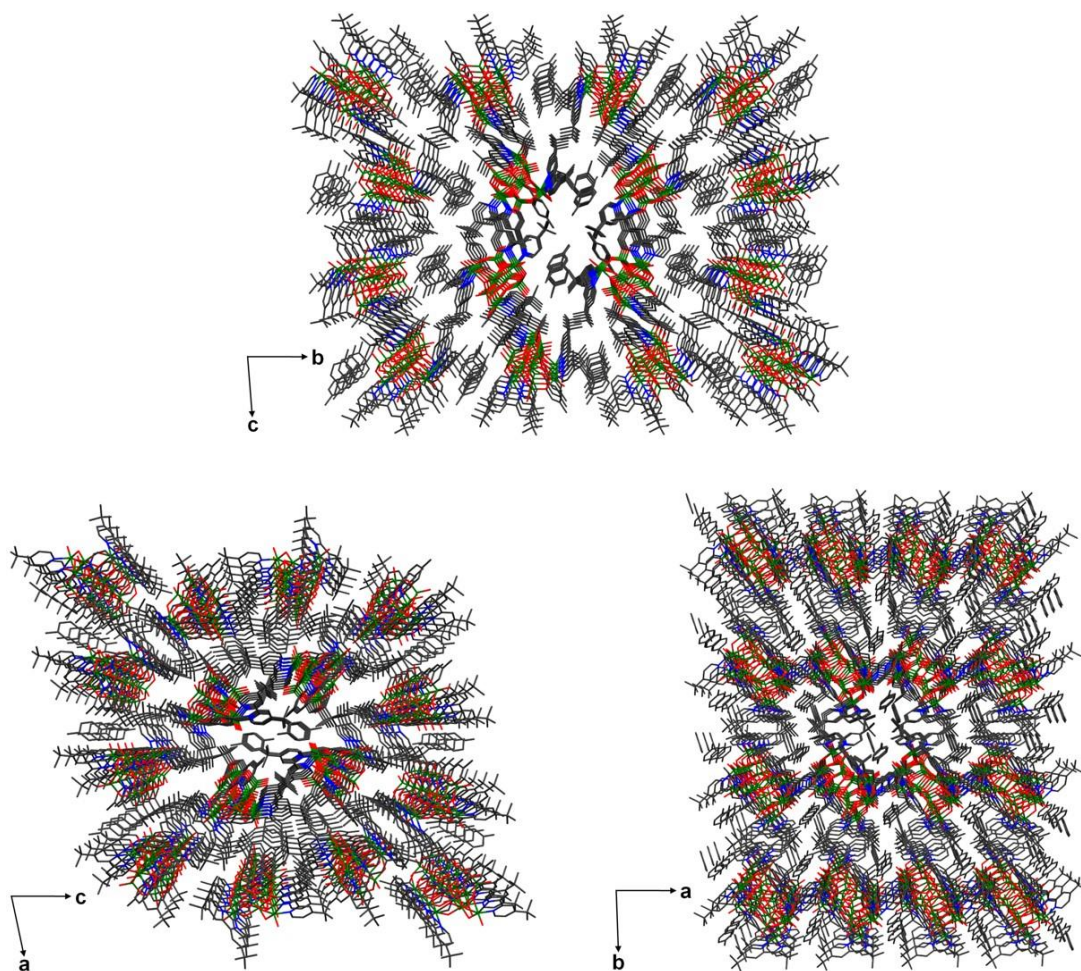


Figure S6. Crystal packing view of $V_8' \cdot 3C_8H_{10}$ along the a -axis (top), b -axis (bottom left), and c -axis (bottom right).

Results of SQUID Measurements

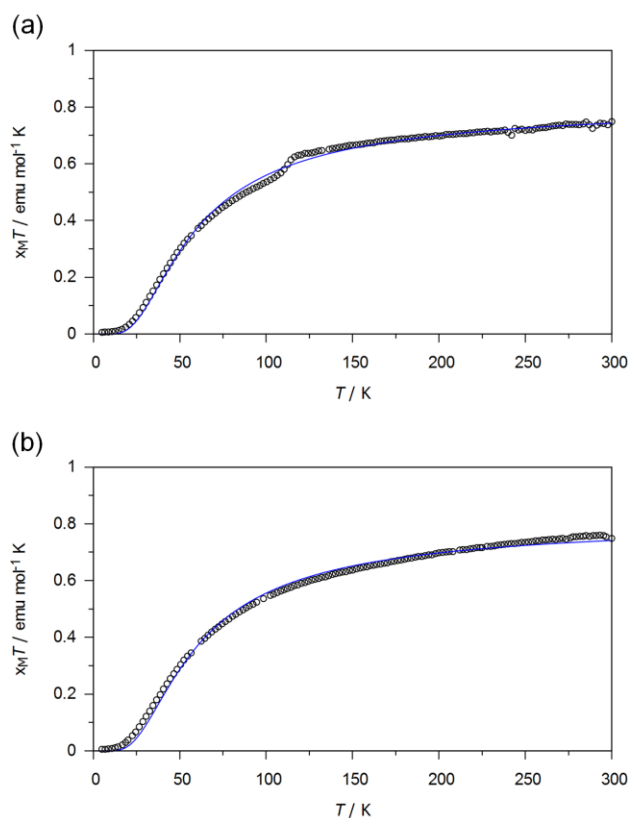


Figure S7. $\chi_M T$ versus T plots for (a) V_4' -Me and (b) V_4' -Et. The solid blue lines represent the theoretical fitting with eq 1 in the manuscript.

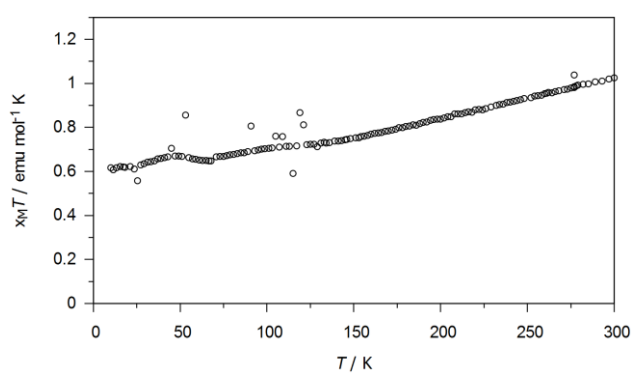


Figure S8. $\chi_M T$ versus T plots for $V_8' \cdot 1.28C_8H_{10}$.

Results of TG-DTA analysis

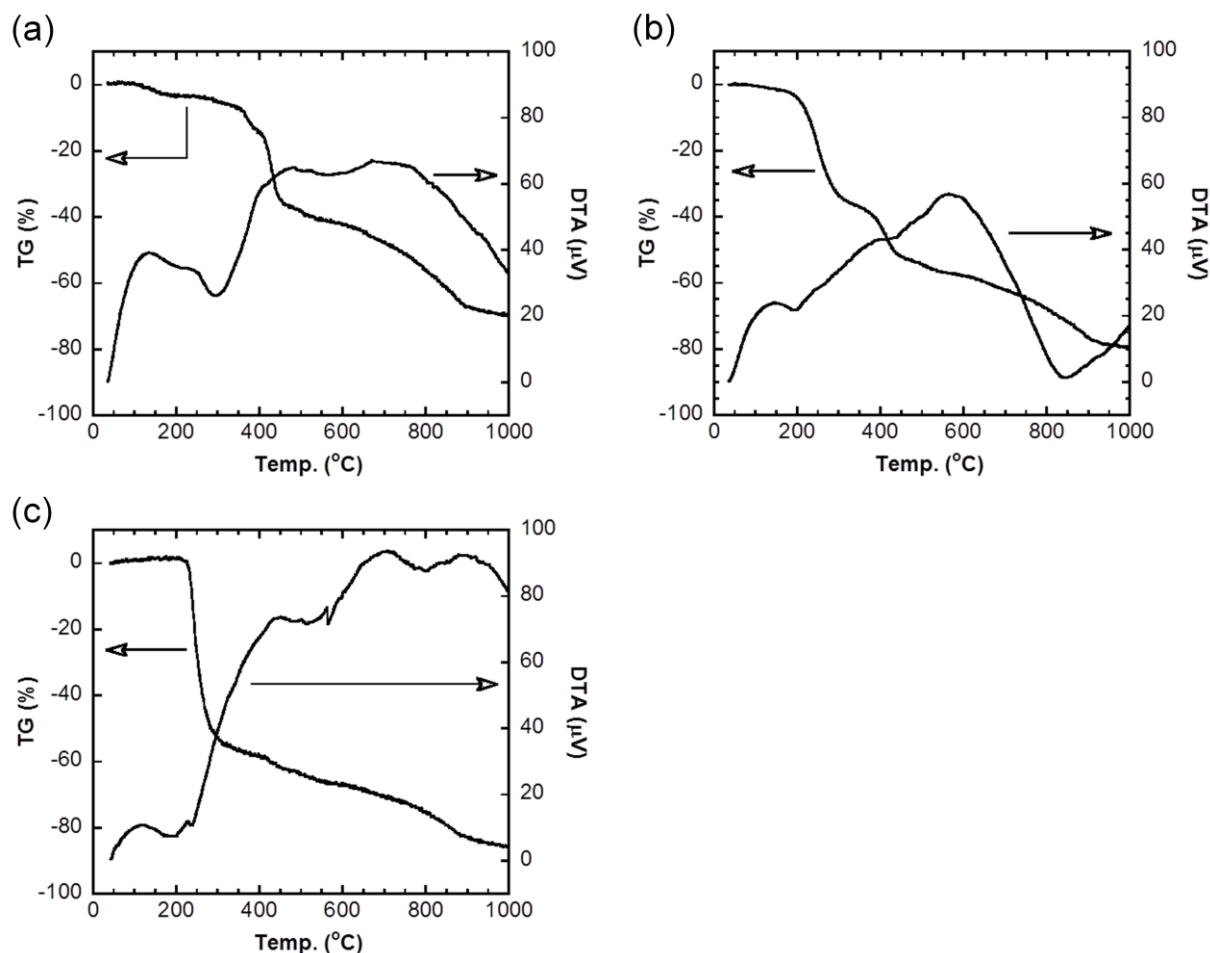


Figure S9. TG-DTA profile of (a) $V_8' \cdot 0.42C_7H_8$, (b) V_4' -Me, and (c) V_4' -Et measured in Ar gas atmosphere. Heating rate: 50 °C/min.

The weight loss of $V_8' \cdot 0.42C_7H_8$ (2.94%) observed at 100–170 °C is attributed to the release of 0.42 toluene molecules (calcd. 2.49%) per empirical formula unit. The next weight loss (32.29%) at 200–460 °C is considered to be due to the loss of two coordinated 4,4'-*t*Bubpy molecules (calcd. 34.51%) (Figure S9a). In addition, the weight losses of V_4' -Me and V_4' -Et were observed at 150–450 °C (50.44%) and at 200–300 °C (54.16%), respectively, which may result from the loss of two 4,4'-*t*Bubpy molecules (calcd. 52.48% for V_4' -Me; calcd. 48.49% for V_4' -Et) (Figures S9b and S9c).

References

- (S1) Bain, G. A.; Berry, J. F. Diamagnetic Corrections and Pascal's Constants. *J. Chem. Educ.* **2008**, *85*, 532–536.
- (S2) Kodama, S.; Taya, N.; Inoue, Y.; Ishii, Y. Synthesis and Interconversion of V₄, V₇, and V₈ Oxide Clusters: Unexpected Formation of Neutral Heptanuclear Oxido(alkoxido)vanadium(V) Clusters [V₇O₁₇(OR)(4,4'-t-Bubpy)₃] (R = Et, MeOC₂H₄). *Inorg. Chem.* **2016**, *55*, 6712–6718.
- (S3) Jacobson, R. A. *REQAB: Private Communication to Rigaku Corporation*; Rigaku Corporation: Tokyo, Japan, 1998.
- (S4) CrystalStructure 4.2.4: *Crystal Structure Analysis Package*, Rigaku Corporation: Tokyo, Japan, 2000–2016.
- (S5) Sheldrick, G. M. A Short History of *SHELX*. *Acta Crystallogr., Sect. A* **2008**, *64*, 112–122.
- (S6) van der Sluis, P.; Spek, A. L. BYPASS: an Effective Method for the Refinement of Crystal Structures Containing Disordered Solvent Regions. *Acta Crystallogr., Sect. A* **1990**, *46*, 194–201.
- (S7) Brese, N. E.; O'Keeffe, M. Bond-Valence Parameters for Solids. *Acta Crystallogr. Sect. B* **1991**, *47*, 192–197.